CaT1 knock-down strategies fail to affect CRAC channels in mucosal-type mast cells

Heike Kahr[1], Rainer Schindl[1], Reinhard Fritsch[1], Barbara Heinze[1], Michael Hofbauer[1], Marlene E. Hack[1], Manuel A. Mörtelmaier[1], Klaus Groschner[2], Ji-Bin Peng[3], Hitomi Takanaga[3], Matthias A. Hediger[3] and Christoph Romanin[1]

[1]*Institute for Biophysics, University of Linz, A-4040 Linz, Austria*
[2]*Institute of Pharmacology and Toxicology, University of Graz, A-8010 Graz, Austria*
[3]*Membrane Biology Program and Renal Divison, Brigham and Women's Hospital, Harvard Institutes of Medicine, Boston, MA 02115, USA*

CaT1, the calcium transport protein 1 encoded by *TRPV6*, is able to generate a Ca^{2+} conductance similar but not identical to the classical CRAC current in mucosal-type mast cells. Here we show that CaT1-derived Ca^{2+} entry into HEK293 cells is effectively inhibited either by expression of various dominant negative N-terminal fragments of CaT1 (N_{334}-CaT1, N_{198}-CaT1 and N_{154}-CaT1) or by antisense suppression. By contrast, the endogenous CRAC current of the mast cells was unaffected by CaT1 antisense and siRNA knockdown but markedly suppressed by two (N_{334}-CaT1, N_{198}-CaT1) of the dominant negative N-CaT1 fragments. Inhibition of CRAC current was not an unspecific, toxic effect, as inward rectifier K^+ and MagNuM currents of the mast cells were not significantly affected by these N-CaT1 fragments. The shortest N_{154}-CaT1 fragment inhibited CaT1-derived currents in mast cells, but failed to inhibit CRAC currents. Thus, the structural requirements of rCaT N-terminal fragments for inhibition of rCaT1 and CRAC channels are different. These results together with the lack of CaT1 antisense and siRNA effects on currents render it unlikely that CaT1 is a component of native CRAC channels in mast cells. The data further demonstrate a novel strategy for CRAC current inhibition by an N-terminal structure of CaT1.

(Resubmitted 11 February 2004; accepted after revision 11 March 2004; first published online 12 March 2004)
Corresponding author C. Romanin: Institute for Biophysics, University of Linz, Altenbergerstr. 69, A-4040 Linz, Austria. Email: christoph.romanin@jku.at

In non-excitable cells generation of inositol trisphosphate (IP_3) by stimulation of phospholipase C subtypes leads to a rapid release of Ca^{2+} from the endoplasmic reticulum store, which is followed by a slow and sustained entry of extracellular Ca^{2+} through store-operated channels (Bootman *et al.* 2001; Putney *et al.* 2001; Venkatachalam *et al.* 2002). A highly calcium-selective store-operated current, termed calcium release activated calcium (CRAC) current (Parekh & Penner, 1997; Lewis, 1999), has been found in mast cells and T-lymphocytes.

Molecular candidates for mammalian store-operated calcium channels are found within the transient receptor potential (TRP) superfamily (Harteneck *et al.* 2000; Clapham *et al.* 2001; Montell, 2001; Gunthorpe *et al.* 2002; Montell *et al.* 2002; Zitt *et al.* 2002) that consists of the TRPC, TRPV and TRPM subgroups. Among these, the calcium transport protein 1 (CaT1) encoded by *TRPV6* has been proposed to manifest pore properties of CRAC channels (Yue *et al.* 2001), particularly the high selectivity for Ca^{2+}. Conflicting results are published, however, on the activation mechanism of CaT1. CaT1 has been found to generate either store-operated (Yue *et al.* 2001; Vanden Abeele *et al.* 2003), or constitutively active conductances (Voets *et al.* 2001; Bodding *et al.* 2002; Cui *et al.* 2002). We have demonstrated that a low level of CaT1 expression leads to store-operated CaT1 currents in mucosal-type rat basophilic leukaemia (RBL) mast cells (line RBL-2H3), whereas high expression levels of CaT1 yield constitutively active currents (Schindl *et al.* 2002). Recently it has been reported (Cui *et al.* 2002) that a pore mutant of CaT1 suppresses CRAC current activation in T-lymphocytes. Beside this and other similarities of CaT1 and CRAC channels, clear differences have been found in the current–voltage relationship of CaT1 and CRAC currents in a divalent free extracellular medium (Schindl *et al.* 2002). Additionally, ion selectivity and unitary conductance of

H. Kahr and R. Schindl contributed equally to the work.

DOI: 10.1113/jphysiol.2004.062653

CaT1 and CRAC channels are different (Voets *et al.* 2001; Prakriya & Lewis, 2002). Nonetheless, these observations still leave the possibility of CaT1 being a subunit of CRAC channels.

In the present study we examined whether rat CaT1 (rCaT1) has a role in CRAC channels of RBL mast cells by an approach that combined RT-PCR, antisense, siRNA and dominant negative knockdown strategies. While the antisense and siRNA approach was effective in eliminating rCaT1-derived currents, CRAC activity was not altered in RBL cells. Among the three N-terminal fragments of rCaT1 that function as a dominant negative species, two of them suppressed rCaT1 activity and were also able to inhibit CRAC currents in mast cells. The shortest N-terminal fragment, however, failed to inhibit CRAC currents while its dominant negative effect on rCaT1 was still preserved. Hence, the structural requirements of rCaT N-terminal fragments for inhibition of rCaT1 and CRAC channels are different.

Methods

Cell culture and molecular cloning

Experiments were performed on a secreting subline (2H3) of RBL mast cells and HEK293 cells cultured according to (Schindl *et al.* 2002). Lymph node carcinoma of the prostate (LNCaP) human prostate cancer epithelial cell line (DSMZ, Germany) were grown in RPMI Medium 1640 supplemented with 10% fetal bovine serum, 2 mM glutamine and 2 U ml^{-1} penicillin and 2 mg ml^{-1} streptomycin, in a humidified atmosphere with 5% CO_2 at 37°C.

The coding region of rCaT1 (accession no. AF160798) was cleaved from pTracer-CMV2 (Invitrogen, USA) and transferred to the plasmid pECFP-C1 or pEYFP-C1 (Clontech, Germany) resulting in the respective amino-terminal tagged clones. For the production of the 334 amino acid (aa), 198 aa and 154 aa N-terminal fragments, three interior restriction sites, *Bsa*AI (334 aa), *Sca*I (198 aa) and *Stu*I (154 aa) were selected. All constructs were subcloned in pTracer-CMV2 and termed N_{334}-rCaT1, N_{198}-rCaT1 and N_{154}-rCaT1. To construct the antisense rCaT1, the complete coding cDNA of rCaT1 was subcloned in pcDNA3 (Invitrogen, USA) in antisense orientation. N_{302}-TRPC3 was cloned from TRPC3 (accession no. U47050) as described (Groschner *et al.* 1998). The integrity of all the constructed clones was confirmed by restriction digests and sequence analysis (VBC Genomics, Austria).

The siRNAs were purchased (Dharmacon Research, USA) and had the following sequences: control siRNA: AAUCAUCUAAGCUGGCUUUGC; and CaT1-siRNA: AACCUGCUGCAGCAGAAGAGG. The latter sequence is fully conserved in both rat and human CaT1.

RT-PCR

The isolated RNA was reverse transcribed using the Super-Script First-Strand Synthesis System (Invitrogen, USA). RNA was quantified using UV light spectrophotometry, and the integrity of the RNA was confirmed by gel electrophoresis. To relate the amount of CaT1 to GAPDH cDNA in the reverse-transcribed samples, real time PCR analysis was performed in the LightCycler System (Roche Molecular Biochemicals, USA) using the following conditions and primers. Each cycle consisted of denaturation for 20 s at 95°C, annealing for 5 s at 65°C (hCaT1), 56°C (rCaT1) or 60°C (human and rat GAPDH), and extension for 25 s at 72°C, with a temperature transition rate of 8°C s^{-1}. Detection of SYBR green fluorescence was performed for 3 s at 86°C (hCaT1), 82°C (rCaT1) or 85°C (GAPDH); primer sequences used for PCR are as follows: hCaT1 forward 5′-AGCCTACATGACCCCTAAGGACG-3′, hCaT1 reverse 5′-GTAGAAGTGGCCTAGCTCCTCGG-3′; rCaT1 forward 5′-CCCGATGAGCTGGGCCATTTCT ATG-3′, rCaT1 reverse 5′-CAGAGTAGAGGTCATCTTGTTGCTG -3′; GAPDH forward 5′-TCACCATCTTCCAGGAGCG-3′, GAPDH reverse 5′-CTGCTTCACCACCTTCTTGA-3′.

Transfection

RBL cells were transfected by electroporation with 20 μg of pTracerCMV2-rCaT1, 40 μg of pTracerCMV2-N-terminal rCaT1 fragments (with 334, 198 or 154 aa), pcDNA3-antisense-rCaT1 or 5.3 μg (200 nM) CaT1-siRNA. Transfection of HEK cells (Schindl *et al.* 2002) was performed using SuperFect (Qiagen, Germany) with 1 μg of pTracerCMV2-rCaT1 or CFP-/YFP-rCaT1, 2–5 μg antisense-rCaT1, 1.25 μg N_{334}-rCaT1, 0.77 μg N198-rCaT1 or N154-rCaT1. Transfected cells were identified by green fluorescent protein (GFP) coexpression encoded in the pTracerCMV2 plasmid or directly via YFP-/CFP-tagged proteins. Specifically, quantification of the number of cells expressing YFP-rCaT1 was carried out by setting a threshold fluorescence intensity level (10% above the background of 60 counts) above which cells were counted as positively expressing cells. Measurements were carried out 24–72 h following electroporation or transfection. For transfection of LNCaP cells, 2 μl Lipofectamin 2000 together with 200 nM CaT1-siRNA or control siRNA was used. Positively tranfected LNCaP cells were identified

by the expression of cotransfected GFP. Recordings were performed 72 h after transfection.

Electrophysiology

Electrophysiological experiments were performed (Schindl *et al.* 2002) at 20–24°C, using the patch-clamp technique (Hamill *et al.* 1981) in the whole-cell recording configuration. Voltage ramps were usually applied every 5 s from a holding potential of 0 mV or +70 mV, covering a range of −90 to +90 mV over 1 s or 200 ms. In RBL mast cells, activation of CRAC currents (observed in all RBL cells) was monitored applying the 1 s voltage ramp at a holding potential of 0 mV and leak-corrected currents were measured at −74 mV. In all recordings that were performed in divalent free (DVF) solutions, a 100 ms ramp (−90 mV to +90 mV) was applied every 2 s from a holding potential of 0 mV according to Voets *et al.* (2001). The pipette solution used to passively deplete intracellular Ca^{2+} stores contained (mM): 145 caesium methane sulphonate, 8 NaCl, 3.5 $MgCl_2$, 10 Hepes, 10 EGTA, pH 7.2. For active store depletion, 20 μM IP_3 and 4.3 mM $CaCl_2$ to maintain 100 nM intracellular Ca^{2+} were added. MagNuM currents of RBL cells were measured without intracellular $MgCl_2$. Pipette solution for inward rectifier currents was (mM): 145 KCl, 1 $MgCl_2$, 10 glucose, 10 Hepes, pH 7.4 (KOH). Bath solution included 140 NaCl, 5 KCl, 1 $MgCl_2$, 2 $CaCl_2$, 10 glucose, 10 Hepes, pH 7.4 (NaOH). Extracellular solution usually consisted of (mM): 145 NaCl, 5 CsCl, 1 $MgCl_2$, 10 Hepes, 10 glucose, 10 $CaCl_2$, pH 7.4. Divalent free (DVF) solution consisted of (mM): 165 NaCl, 5 CsCl, 10 Hepes, 10 glucose, 10 EDTA, pH 7.4 (CsOH).

Fluorescence resonance energy transfer (FRET)

Tranfected HEK cells grown on coverslips for 1 day were transferred to an extracellular solution identical to the bath solution used to record inward rectifier currents (see above). A QLC100 Real-Time Confocal System (VisiTech Int., UK) was used for recording images and was connected to two Photometrics $CoolSNAP_{HQ}$ monochrome cameras (Roper Scientific, USA). This system was attached to an Axiovert 200M microscope (Zeiss, Germany) in conjunction with an argon ion multi-wavelength (457, 488, 514 nm) laser (Laser Physics Inc., USA). The wavelenghts were selected by an Acousto Optical Tuneable Filter (VisiTech Int., UK). The dual port adapter contains a 505lp dichroic, a 485/30 cyan emission filter and a 535/50 yellow emission filter (Chroma Technology Corp., USA). MetaMorph 5.0 software (Universal Imaging Corp.) was used to acquire images and to control the confocal system.

The FRET image has to be corrected due to a cross-talk from one channel to the other. For this, the corrected FRET image (nFRET) was calculated after background subtraction using a custom-made software integrated in MatLab 6 according to the following equation (Xia & Liu, 2001):

$$\mathrm{nFRET} = \frac{(I_{\mathrm{FRET}} - (\mathrm{I_{YFP}})(\mathrm{Cal_{YFP}}) - (\mathrm{I_{CFP}})(\mathrm{Cal_{CFP}}))}{\sqrt{\mathrm{I_{YFP}I_{CFP}}}}$$

denotes the background corrected intensity of the FRET image (excitation 457 nm, emission 535 nm), I_{YFP} the background corrected intensity of the YFP image (excitation 514 nm, emission 535 nm) and I_{CFP} the background corrected intensity of the CFP image (excitation 457 nm, emission 485 nm). The $\mathrm{Cal_{CFP}}$ factor and the $\mathrm{Cal_{YFP}}$ factor were obtained from experiments where only CFP or YFP was expressed ($\mathrm{Cal_{YFP}} = I_{\mathrm{FRET}}/I_{\mathrm{YFP}} = 0.4$; $\mathrm{Cal_{CFP}} = I_{\mathrm{FRET}}/I_{\mathrm{CFP}} = 0.4$).

Ca^{2+} fluorescence measurements

RBL cells were grown on coverslips for 1 day and loaded with fura-2/AM (1 μM) for 20 min at 20°C in Dulbecco's modified Eagle's medium (see Cell culture and molecular cloning) and washed three times; dyes were allowed to deesterify for 15 min at 20°C. Coverslips were transferred to an extracellular solution without Ca^{2+} and mounted at an inverted Axiovert 100 TV microscope (Zeiss, Germany). Excitation of Fura-2 was performed at 340 nm and 380 nm, and Ca^{2+} measurements are shown as 340/380 ratios of both GFP and untransfected RBL cells.

Statistics

Results are presented as means ± S.E.M. calculated for the indicated number of experiments. Student's two-tailed *t* test was used for statistical comparison considering differences statistically significant at $P < 0.05$.

Results

rCaT1 has been proposed to manifest pore properties of CRAC channels, particularly due to its high selectivity for Ca^{2+} (Yue *et al.* 2001). A quantitative comparison of the levels of CaT1 mRNA expression in RBL and LNCaP cells yielded GAPDH-normalized values ((CaT1/GAPDH) × 10^3) of 0.000000 (below the detection limit) and 3.797823, respectively, confirming CaT1 expression in LNCaP (Peng *et al.* 2001; Wissenbach *et al.*

2001). The expression of endogenous rCaT1 in RBL mast cells may have also failed biochemical detection by Northern blot analysis (Bodding *et al.* 2002) probably due to extremely low mRNA levels, although the rCaT1 clone used in this study was derived from the RBL mast cells (Yue *et al.* 2001).

Hence, to ultimately evaluate a contribution of rCaT1 protein to CRAC activity in RBL mast cells, we alternatively employed antisense (AS) and siRNA knock-down strategies to inhibit rCaT1 protein expression. We initially started with an antisense (AS) approach to inhibit rCaT1 protein expression. The efficiency of the constructed rCaT1-antisense (rCaT1-AS) was assessed in HEK cells by a reduction in the expression of yellow fluorescent protein (YFP)-tagged rCaT1 (Fig. 1*A*) or in the level of rCaT1-derived currents (Fig. 1*B* and *C*). The amount of YFP-rCaT1 was significantly reduced by coexpression of rCaT1-AS (2-fold or 5-fold excess; Fig. 1*A*). Consistently, coexpression of rCaT1 and rCaT1-AS led to a significant reduction of the constitutively active rCaT1-derived currents in HEK cells substantiating the efficiency of our rCaT1-AS probe. Specificity of this probe was confirmed by a small yet not significant inhibition of human calcium transport protein 1 (hCaT1)-derived currents (Fig. 1*D* and *E*).

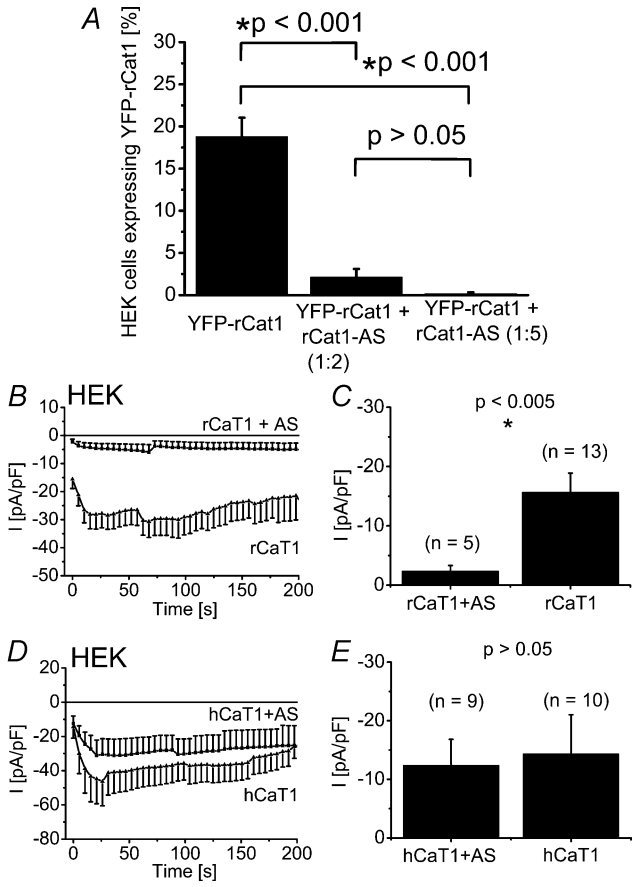

Figure 1. Expression of rCaT1 antisense reduces rCaT1 protein expression and rCaT1-derived currents in HEK cells
A, the percentage of YFP-rCaT1 transfected cells was significantly reduced when rCaT1-AS was coexpressed in a 2-fold or 5-fold excess, estimated from proportion of YFP-fluorescent cells. Each transfection was performed in triplicate and of each, 3–17 images were analysed. *B* and *D*, time course of constitutively active, whole-cell inward currents of rCaT1 (*B*) and hCaT1 (*D*) transfected HEK cells and those cotransfected with rCaT1-AS (*B* and *D*). Co-expression of rCaT1-AS significantly reduced rCaT1-derived inward currents recorded immediately after obtaining whole-cell configuration (*C*), whereas hCaT1 currents were not significantly altered (*E*).

In RBL mast cells, expression of rCaT1 leads to the formation of store-operated rCaT1 channels that are activated similar to endogenous CRAC currents, resulting in an about twofold increase in current density (Schindl *et al.* 2002). When rCaT1-AS was coexpressed with rCaT1 cDNA in these mast cells, a reduction of Ca^{2+} inward current was observed to the current level usually reached by CRAC (Fig. 2*A*–*D*) indicating that endogenous CRAC currents remained unaffected. The complete suppression of rCaT1-derived currents by rCaT1-AS was substantiated by analysis of current–voltage relationships in divalent free solution (Voets *et al.* 2001; Schindl *et al.* 2002) that enabled clear differentiation between CRAC and rCat1 currents (Fig. 2*D*). The fingerprint of rCaT1 (Voets *et al.* 2001; Schindl *et al.* 2002) represented by a negative slope in the current–voltage relationship (arrow in Fig. 2*D*) was absent in CRAC currents from control RBL mast cells and was abolished in cells cotransfected with both rCaT1 and rCaT1-AS (Fig. 2*D*).

As an alternative second approach, siRNA against CaT1 was employed to knock-down potential endogenous CaT1 (Fig. 3). LNCaP cells that posses a store-operated Ca^{2+} channel partially involving CaT1 (Skryma *et al.* 2000; Vanden Abeele *et al.* 2003) were initially used to estimate optimal siRNA concentrations based on a reduction of ^{45}Ca influx (data not shown). Then, effective concentrations of 200 nM siRNA were examined on depletion-activated endogenous CaT1 currents in LNCaP cells (Fig. 3*A* and *B*) resulting in a significant reduction of these Ca^{2+} currents when compared to the effect of control siRNA consistent with Vanden Abeele *et al.* (2003). However, the same siRNA failed to reduce CRAC currents in RBL mast cells (Fig. 3*C* and *D*), although the current derived from rCaT1 overexpressed in these cells was significantly reduced to the level of endogenous CRAC current (Fig. 3*E* and *F*). Consistently, efficacy of siRNA on overexpressed YFP-tagged rCaT1 in RBL cells was observed by both an about 2.3-fold reduction in cells exhibiting an average fluorescence intensity above

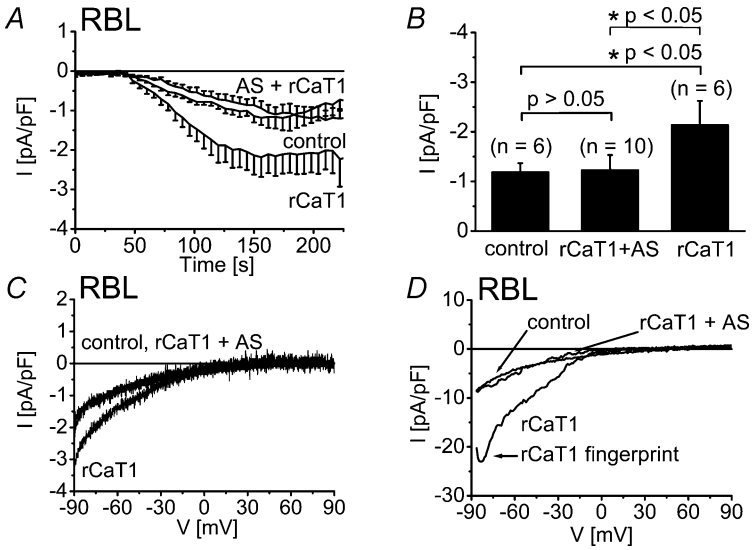

Figure 2. Expression of rCaT1-AS in RBL mast cells did not reduce CRAC current
RBL cells were mock-transfected or transfected with either rCaT1 or both rCaT1 plus rCaT1-AS. *A*, time courses of whole-cell inward currents induced by passive (10 mM EGTA) store depletion. *B*, transfection of rCaT1 significantly enhanced maximum inward currents in RBL cells. rCaT1 plus rCaT1-AS cotransfected RBL cells exhibited inward currents that were not significantly different from those of mock-transfected (control) RBL cells. Current traces evoked in divalent containing (*C*) or divalent free (*D*) extracellular solution are shown for mock-transfected (control), rCaT1 and rCaT1 plus rCaT1-AS transfected RBL cells. Current traces of mock-transfected (control) and rCaT1 plus rCaT1-AS completely overlap (*C*).

background and an about 10-fold reduction in their average fluorescence intensity level when compared with control (data not shown). Thus, the lack of effect of CaT1 antisense and siRNA knockdown strategies on CRAC currents suggests that rCaT1 is not a component of the native CRAC current in RBL mast cells.

In a third approach we tested for an effect of dominant negative rCaT1 species on CRAC activity in RBL mast cells. Based on the finding that TRPV proteins yield a functional channel associated with their ability to form a tetrameric structure (Kedei *et al.* 2001; Hoenderop *et al.* 2003) via their amino (N)-terminus (Xu *et al.* 1997),

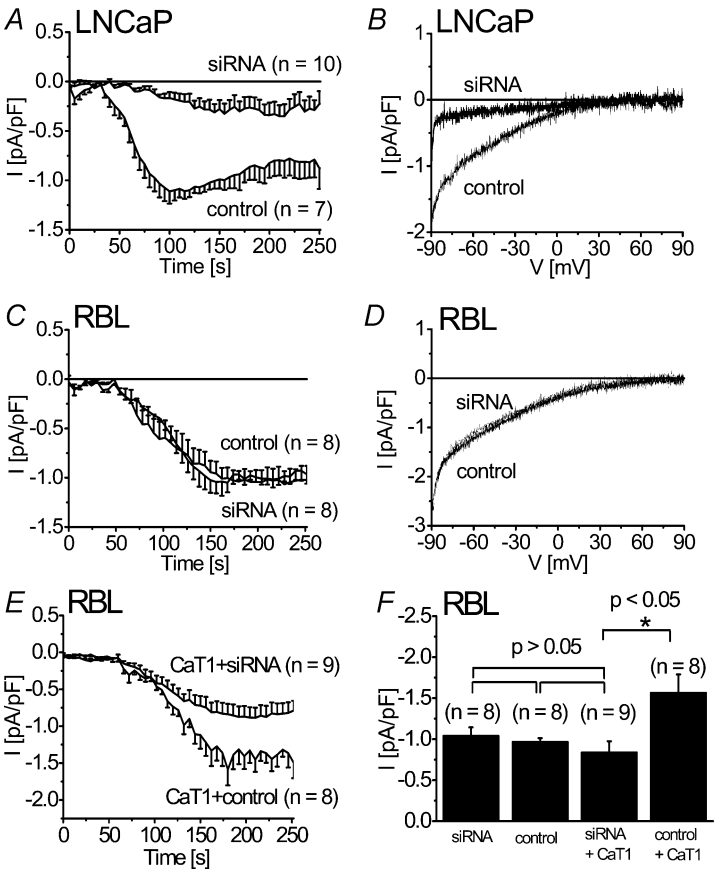

Figure 3. siRNA against CaT1 suppressed store-operated Ca^{2+} inward currents in LNCaP cells and overexpressed CaT1 in RBL cells but not endogenous CRAC currents
LNCaP (*A* and *B*) or RBL cells (*C*–*E*) were either transfected with CaT1-siRNA and GFP, control siRNA and GFP (*C* and *D*) or rCaT1 with siRNA or control siRNA (*E*). Time courses are shown of whole-cell inward currents of LNCaP cells (*A*) or RBL mast cells (*C* and *E*) activated through passive (10 mM EGTA) store depletion. A representative current–voltage relationship is shown for both rCaT1 siRNA or control siRNA transfected LNCaP cells (*B*) and RBL cells (*D*). CaT1 overexpressed in RBL cells is significantly suppressed by siRNA, while endogenous CRAC currents are unaffected by CaT1 siRNA or control siRNA (*F*).

we first confirmed *in vivo* assembly of rCaT1 proteins, and then later on examined the interaction capability of expressed N-terminal fragments of CaT1. Thus rCaT1 was labelled at the N-terminus with either cyan fluorescent protein (CFP) or yellow fluorescent protein (YFP), and both differentially labelled proteins were coexpressed at a 1 : 1 molar ratio in HEK cells. Assembly of rCaT1 proteins was evaluated from fluorescence resonance energy transfer (FRET) measurements (Fig. 4). The corrected FRET image (Fig. 4*A*, upper panel d; nFRET, see Methods) depicts higher nFRET values for HEK cells expressing both CFP-rCaT1 and YFP-rCaT1 compared to control cells expressing CFP and YFP-rCaT1 (Fig. 4*C*). The statistical evaluation of average nFRET values indicated significantly higher nFRET when both rCaT1 proteins are labelled (Fig. 4*C*), in line with the formation of rCaT1 tetramers (Hoenderop *et al.* 2003). This tetramer formation might involve the N-terminus of rCaT1 as evident from FRET experiments with coexpressed CFP-/YFP-labelled N-termini of rCaT1 in HEK cells (Fig. 4*B*). As compared to control cells, significantly higher nFRET values were calculated when both N-termini (N_{198}-rCaT1, see below) were labelled (Fig. 4*B* and *D*) pointing to an interacting capability inherent to the N-terminal portion of rCaT1.

Additional experiments were carried out to determine FRET between N_{198}-rCaT1 and rCaT1 proteins labelled by CFP and YFP, respectively. Interestingly, we could not detect a significant (t test, $P > 0.05$) difference between control CFP + YFP-rCaT1 ($n = 9$) and CFP-N_{198}-rCaT1 + YFP-rCaT1 ($n = 11$) nFRET average values when calculated from whole cell areas. To reveal a possible weak interaction between CFP-N_{198}-rCaT1 and YFP-rCaT1, we performed another type of analysis based on the comparison of those nFRET values in these distributions which are lying above an upper limit that comprises 95% of nFRET values of the control distribution (CFP + YFP-rCaT1). Here we determined that the probability of detecting nFRET is about 110-fold and 70-fold higher with interacting N-terminal fragments and whole CaT1

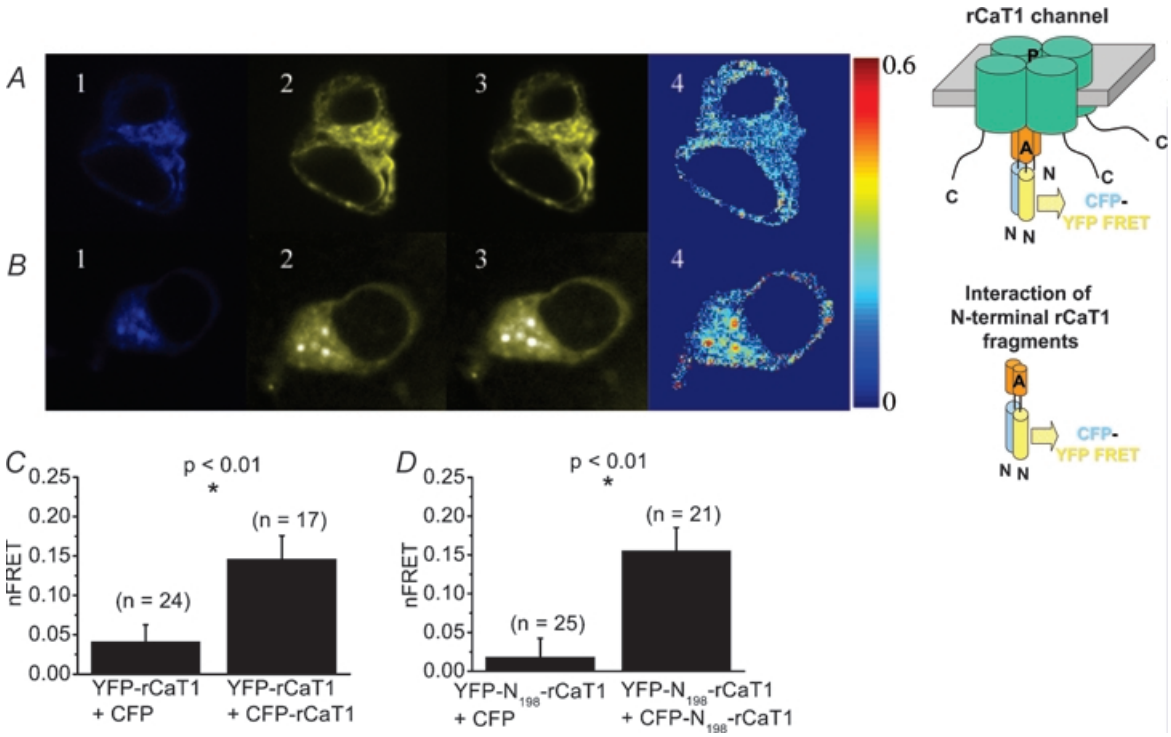

Figure 4. *In vivo* assembly of CFP-/YFP-labelled rCaT1 proteins and of their CFP-/YFP-labelled N-terminal fragments

HEK cells were cotransfected with CFP- and YFP-labelled CaT1 (*A*) or CFP- and YFP-labelled N-terminal rCaT1 fragments (*B*). Representative CFP_{excit}/CFP_{emis} (1), CFP_{excit}/YFP_{emis} (2, FRET), and YFP_{excit}/YFP_{emis} (3) images and the corrected FRET image (4, nFRET) are shown in *A* and *B*. For control, transfection was carried out with CFP and YFP-rCaT1 (*C*) or CFP and YFP-N_{198}-rCaT1 (*D*). On average, CFP-/YFP-rCaT1 (*C*) and CFP-/YFP-N_{198}-rCaT1 (*D*) cotransfected cells showed a significantly higher nFRET when calculated for the whole HEK cell in comparison to control. *n* denotes the number of cells analysed.

proteins, respectively, than with N-terminal fragment + CaT1 proteins (data not shown). This weak and less frequently occurring interaction of N-terminal rCaT1 fragment with rCaT1 compared to that of N-terminal rCaT1 fragments is consistent with results from Montell's group (Xu *et al.* 2001) where a much stronger interaction has been reported for the N-terminal fragments of TRP-related protein (MLSN-S) in comparison to that of the N-terminal fragment (MLSN-S) with the whole TRP-related protein (MLSN-L).

Based on these findings and on previous reports (Xu *et al.* 1997; Groschner *et al.* 1998) that have demonstrated TRP protein interactions via the N-terminal strand, we tested for a potential dominant negative effect of the N-terminus of rCaT1 which might substitute for rCaT1 in a tetramer resulting in formation of non-functional rCaT1 channels. For this, we coexpressed the N-terminus of rCaT1 (N_{334}-rCaT1) together with rCaT1 in HEK cells and compared their inward currents with those of control HEK cells expressing only rCaT1. The N_{334}-rCaT1 significantly suppressed rCaT1-derived Ca^{2+} inward currents (Fig. 5*A* and *B*) thus representing a tool with an efficient dominant negative effect on CaT1-containing channels. Consistently, expression of a CaT1 mutant where the N-terminus was

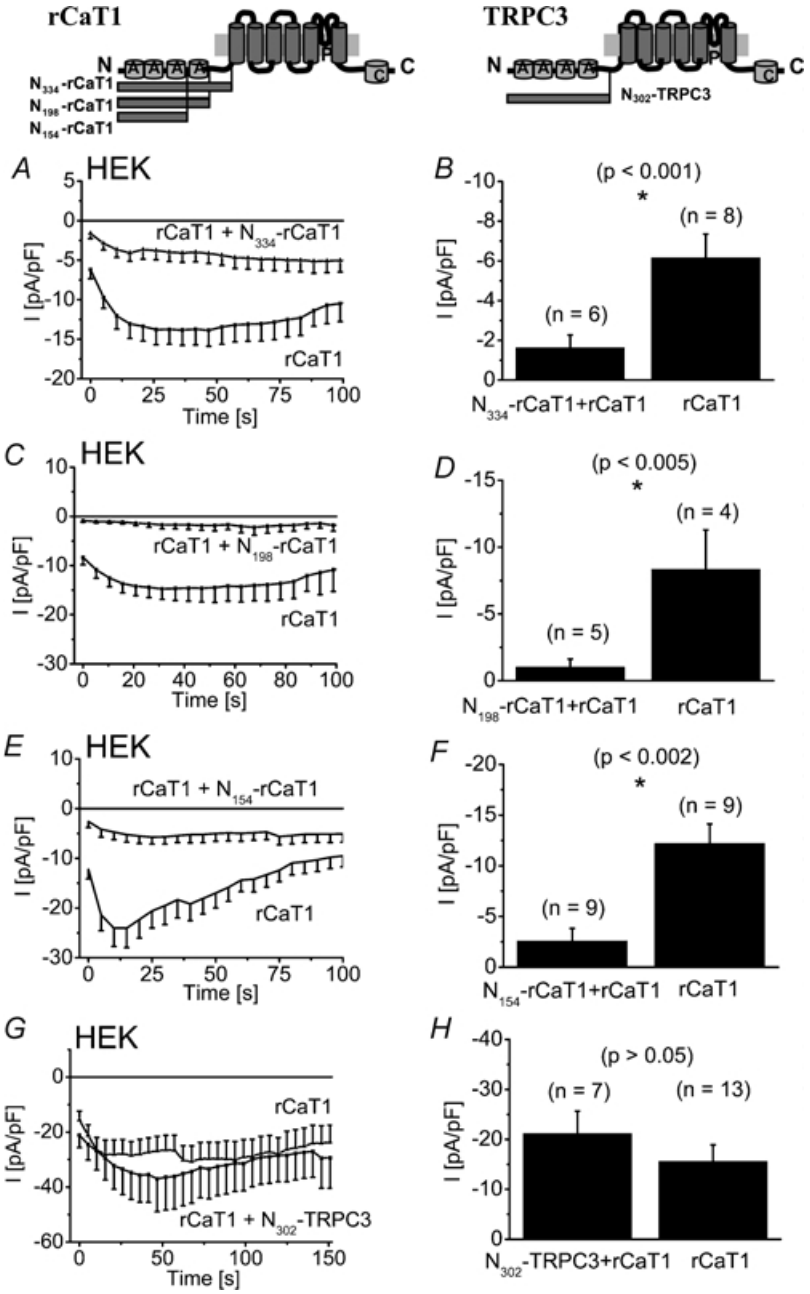

Figure 5. N-terminal fragments of rCaT1 reduce rCaT1-derived inward currents in HEK293 cells
Illustrations in the upper panel depict the structure of rCaT1 (left) and TRPC3 (right), including N-terminal ankyrin-like repeats marked as A, transmembrane domains in grey, the pore region marked as P and a calmodulin binding sequence marked as C. Time courses are shown of constitutively active inward currents from HEK cells cotransfected with rCaT1 and with N_{334}–rCaT1 (*A*), N_{198}-rCaT1 (*C*), or N_{154}-rCaT1 (*E*) in comparison with rCaT1 transfected HEK cells. Significantly smaller inward currents were detected in N_{334}–rCaT1 (*B*), N_{198}-rCaT1 (*D*), or N_{154}-rCaT1 (*F*) cotransfected HEK293 cells. *G*, time course of inward currents from HEK cells cotransfected with rCaT1 and N_{302}-TRPC3 compared to rCaT1 transfected cells. *H*, N_{302}-TRPC3 cotransfected HEK cells did not show a significantly different inward current compared to rCaT1-transfected HEK cells.

deleted failed to produce detectable currents, supporting its importance in the formation of functional channels (data not shown). To further narrow the domain within the N_{334}-rCaT1, shorter N-termini of rCaT1 (N_{198}-rCaT1, N_{154}-rCaT1) were generated and were found to be similarly effective as the longer form in suppressing rCaT1-derived currents (Fig. 5*C–F*). These results localize the dominant negative domain of the N-terminus of rCaT1 within the first 154 amino acids. The mechanism(s) responsible for the dominant negative effect of N-terminal rCaT1 fragments will be the focus of further studies, as the interaction between whole rCaT1 and N_{198}-rCaT1 based on

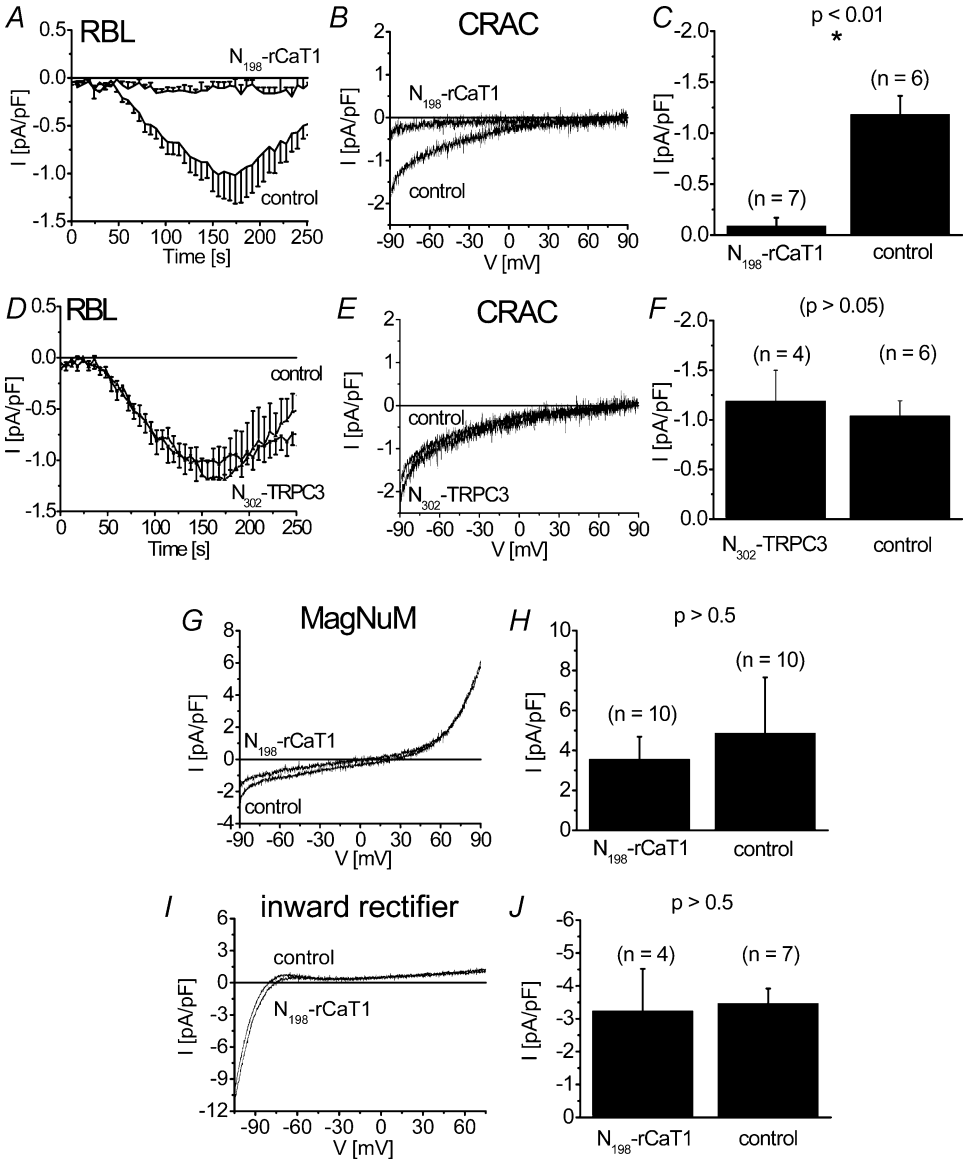

Figure 6. N_{198}-rCaT1 inhibits CRAC channel activity in RBL mast cells

RBL cells transfected with N_{198}-rCaT1 (*A–C*) and N_{302}-TRPC3 (*D–F*) as well as mock-transfected RBL cells are stimulated by passive (10 mM EGTA) store depletion to evoke CRAC currents. Time courses of whole-cell inward currents are shown in *A* and *D*. Representative current–voltage relationships of CRAC currents are shown for N_{198}-rCaT1 (*B*) or N_{302}-TRPC3 (*E*) transfected cells in comparison to control. *C*, inward currents of N_{198}-rCaT1 transfected RBL cells are significantly smaller than CRAC currents of mock-transfected RBL cells (control). *F*, RBL cells transfected with N_{302}-TRPC3 did not show significantly different CRAC currents when compared with mock-transfected RBL cells. N_{198}-rCaT1 did not affect endogenous MagNuM (*G*) and K^+ inward rectifyer (*I*) currents in RBL cells. Maximum currents of MagNuM (*H*; determined at +74 mV) and K^+ inward rectifier (*J*; determined at −80 mV) in N_{198}-rCaT1 transfected cells were not significantly different from mock-transfected cells.

FRET analysis as mentioned before seems to be weak despite the strong dominant negative effect. Consistently, a strong dominant negative effect was observed for the N-terminal fragment (MLSN-S) with the whole TRP-related protein (MLSN-L) despite a weak interaction (Xu *et al.* 2001). Four ankyrin-like repeats have been identified within the 198 amino acids (Peng *et al.* 1999) that might contribute to the observed dominant negative effect of the N_{198}-rCaT1. To examine for a possible involvement of the ankyrin-like repeats, the N-terminus of TRPC3 (N_{302}-TRPC3) exhibiting four such repeats was employed as a surrogate. Co-expression of N_{302}-TRPC3 with rCaT1, however, did not significantly suppress rCaT1-derived currents (Fig. 5*G* and *H*). This finding renders it unlikely that ankyrin-like repeats are responsible for the observed dominant negative effect of the various N-terminal fragments and favours a role of these fragments in disturbing the formation of functional channels.

Thus having established the dominant negative effect of the N-terminal rCaT1 fragments on rCaT1-derived currents, we examined their effects on the endogenous CRAC currents in RBL mast cells. In contrast to the results of the rCaT1 antisense and siRNA experiments, expression of the N_{334}-rCaT1 (data not shown) and N_{198}-rCaT1 fragments substantially suppressed activation of endogenous CRAC (Fig. 6*A–C*). This suppression was observed when activation of CRAC currents was induced either by passive (10 mM EGTA; Fig. 6*A–C*) or active (20 μM IP_3 +100 nM Ca^{2+}, data not shown, $P < 0.05$, $n = 6$) store depletion. Additionally, the store-operated Ca^{2+} current obtained by rCaT1 expression in RBL cells (Schindl *et al.* 2002) was similarly depressed by N_{198}-rCaT1 (data not shown, $P < 0.001$, $n = 6$). To assess that the blocking effect of N_{198}-rCaT1 is not an unspecific impairment of cell function, we tested its effect on the inward rectifier K^+ (Wischmeyer *et al.* 1995) and MagNuM (Kozak *et al.* 2002) currents of RBL mast cells (Fig. 6*G–J*). Both currents were not significantly affected by N_{198}-rCaT1. Hence both the N_{334}-rCaT1 and the N_{198}-rCaT1 function as inhibitors of CRAC activity in RBL mast cells.

Further, expression of the N_{302}-TRPC3 fragment affected neither the activation nor the amount of endogenous CRAC currents in RBL mast cells (Fig. 6*D–F*) suggesting that the ankyrin-like repeats play a minor role in the inhibition of CRAC activity by the longer N-rCaT1 fragments.

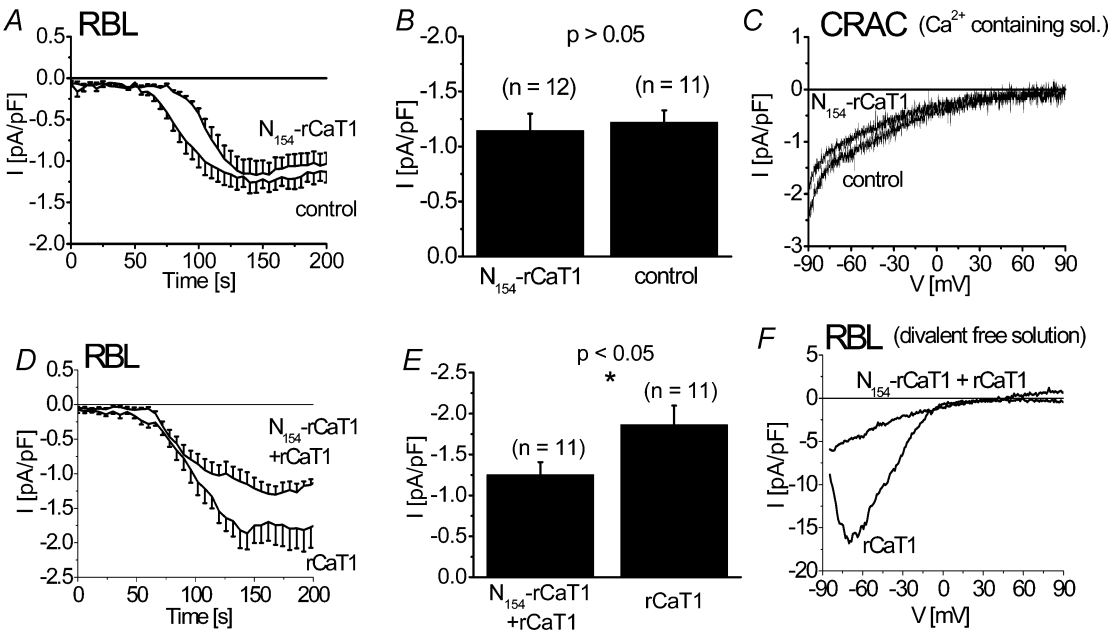

Figure 7. N_{154}-rCaT1 significantly inhibited overexpressed rCaT1 currents while CRAC currents are unaffected in RBL mast cells

RBL cells transfected with N_{154}-rCaT1 (*A–C*) or N_{154}-rCaT1 and rCaT1 (*D–F*) as well as mock-transfected RBL cells are stimulated by passive (10 mM EGTA) store depletion. Time courses of whole-cell inward currents are shown in *A* and *D*. Representative current–voltage relationships of CRAC currents are shown for N_{154}-rCaT1 (*B*) or N_{154}-rCaT1 and rCaT1 (*E*) transfected cells in comparison to control. Current–voltage relationships in a Ca^{2+} containing extracellular solution are compared for N_{154}-rCaT1 and mock-transfected RBL mast cells (*C*) and in a divalent free solution for transfected N_{154}-rCaT1 and cotransfected N_{154}-rCaT1 and rCaT1 RBL mast cells (*F*).

In contrast to the two longer N-terminal fragments of rCaT1, expression of N_{154}-rCaT1 in RBL mast cells clearly failed to affect the amount of CRAC activated (Fig. 7*A*–*F*). A small delay in the activation was observed in N_{154}-rCaT1 expressing cells (Fig. 7*A*), but CRAC characteristics such as the current increase and its permeability properties as judged from the current–voltage relationships remained unchanged. Similar results were obtained when rCaT1 was coexpressed with N_{154}-rCaT1 in RBL mast cells where store-operated rCaT1-derived currents were inhibited while endogenous CRAC currents remained unaffected (Fig. 7*D*–*F*). Hence, this N_{154}-rCaT1 construct unequivocally discriminates between rCaT1 and CRAC currents.

To study the effects of the N-terminal fragments of rCaT1 in a more physiological context, Ca^{2+} fluorescence measurements (Fura-2) were performed on RBL mast cells stimulated by the Ca^{2+}-ATPase inhibitor 2,5-di-t-butyl-1,4-hydrochinone (BHQ) (Fig. 8*A*, *B* and *E*–*H*) or immunologically by IgE plus antigen (Fig. 8*C* and *D*). RBL cells were initially stimulated in nominally Ca^{2+} free solution followed by the addition of Ca^{2+}-containing extracellular solution which allows separation of release of intracellular Ca^{2+} from the entry of extracellular Ca^{2+}. Release of Ca^{2+} from intracellular stores induced by BHQ was not altered by expression of N_{198}-rCaT1 in RBL mast cells suggesting a target downstream of store depletion. Indeed, store-operated Ca^{2+} entry over the plasma membrane initiated by re-addition of extracellular Ca^{2+} was markedly reduced in these cells (Fig. 8*A* and *B*) consistent with the observed inhibition of CRAC currents as detected in electrophysiological experiments. Further,

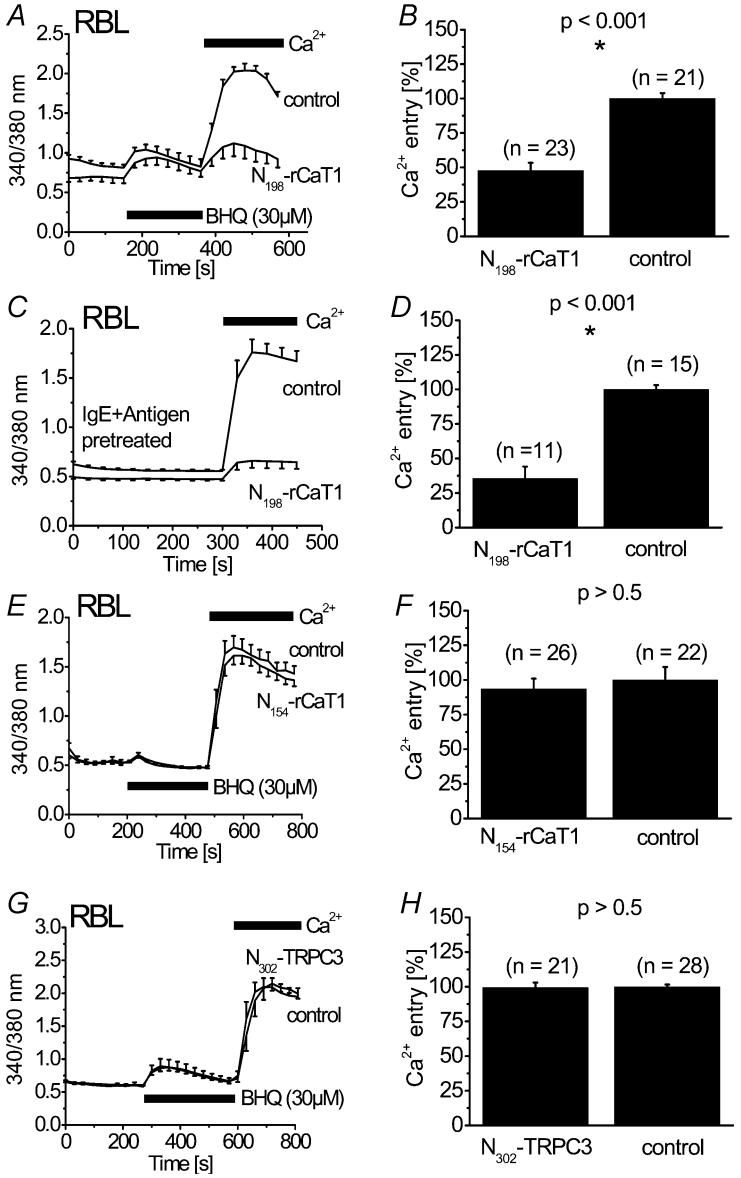

Figure 8. N_{198}-rCaT1 in contrast to N_{154}-rCaT1 inhibits Ca^{2+} entry in RBL mast cells

Intracellular [Ca^{2+}] of Fura-2 loaded cells was initially monitored in a nominally Ca^{2+} free solution followed by addition of extracellular Ca^{2+}. RBL cells mock-transfected (control) or transfected with N_{198}-rCaT1 (*A*–*D*), N_{154}-rCaT1 (*E* and *F*) or N_{302}-TRPC3 (*G* and *H*) were stimulated with 30 μM BHQ (*A* and *B*, and *E*–*H*) or pretreated with IgE plus antigen (*C* and *D*). Adddition of 2 mM external Ca^{2+} revealed a significantly reduced rate of calcium entry in N_{198}-rCaT1 transfected cells (*A*–*D*) compared to control cells, whereas neither N_{154}-rCaT1 (*E* and *F*) nor N_{302}-TRPC3 (*G* and *H*) significantly altered Ca^{2+} entry. Data shown in (*A*, *C*, *E* and *G*) are from representative experiments with 8–10 cells under each condition. Results in *B*, *D*, *F* and *H* were from 3 to 5 independent transfections.

Ca^{2+} entry induced by immunological stimulation of RBL mast cells was inhibited by N_{198}-rCaT1 (Fig. 8*C* and *D*). Moreover, the intracellular Ca^{2+} concentration in cells expressing N_{198}-rCaT1 was slightly lower in nominally Ca^{2+} free solution as compared to control cells (Fig. 8*A* and *C*) suggesting inhibition of basal Ca^{2+} entry. However, Ca^{2+} entry in N_{154}-rCaT1 expressing RBL cells, occurred to a similar extent as in mock-transfected cells (Fig. 8*E* and *F*) in accordance with the electrophysiological experiments.

Expression of the N_{302}-TRPC3 affected neither Ca^{2+} release nor Ca^{2+} entry (Fig. 8*G* and *H*).

Discussion

Yue *et al.* (2001) have suggested that CaT1 manifests the pore properties of CRAC channels and is activated by store depletion in CHO cells. In accordance with the concept of a link between CaT1 channels and intracellular Ca^{2+} stores, we have recently demonstrated store-dependent activation of CaT1 when expressed in RBL mast cells (Schindl *et al.* 2002). However, monovalent currents through CaT1 channels display a current–voltage relationship distinct from endogenous CRAC currents (Voets *et al.* 2001; Schindl *et al.* 2002), indicating that CRAC and CaT1 pore structures are not identical, which is further supported by a different ionic selectivity and single channel conductance (Voets *et al.* 2001; Prakriya & Lewis, 2002). Recently, a contribution of CaT1 to CRAC currents has been again suggested (Cui *et al.* 2002) as inferred from the suppression of endogenous CRAC activity in Jurkat T-lymphocytes when a pore mutant of CaT1 impermeable to Ca^{2+} is expressed. These authors have concluded that CaT1 is at least in part responsible for the native CRAC currents. The results of our present study shed light on this apparent discrepancy. The lack of effect of rCaT1 antisense and siRNA on endogenous CRAC currents in RBL mast cells together with an rCaT1 mRNA level below the detection limit as observed in this study renders it unlikely that rCaT1 is a subunit of native CRAC channels. However, we cannot completely exclude that knock-down strategies might be less efficient if the turnover of endogenous CaT1 as a component of CRAC channel complex is much slower than that of overexpressed CaT1 preventing the efficacy of our knock-down/dominant negative approaches.

The inhibition of CRAC currents in Jurkat T-lymphocytes by an expressed pore mutant of CaT1 (Cui *et al.* 2002) might be related to its interaction with CRAC channel proteins or within the activation pathway of both CRAC and CaT1 channels. We observed (unpublished results) a lack of effect of rCaT1 siRNA on Ca^{2+} entry in Jurkat cells in accordance with the results in RBL mast cells, and a similar inhibition with the N_{198}-fragment of rCaT1, possibly assigning inhibition of CRAC currents by the expressed pore mutant of CaT1 (Cui *et al.* 2002) to structures in its N-terminus. Three N-terminal rCaT1 fragments (N_{334}, N_{198} and N_{154}) functioned as dominant negatives for rCaT1. While the N_{334}- and N_{198}-terminal fragments of rCaT1 were also identified as inhibitors of CRAC activity, the smallest N_{154}-terminal fragment was ineffective indicating divergent structural requirements for CRAC and rCaT1 inhibition. Alternatively, the structural constraints of N-terminal fragments to act as dominant negative species might depend on the assembly of CaT1 in a homotetrameric or heterotetrameric form. The latter assembly could require the longer N-terminal fragments of CaT1 for inhibition, while the shortest N_{154}-terminal strand might not posses an affinity high enough to disrupt a heteromultimeric CRAC/CaT1 channel complex. Nevertheless, store-operated Ca^{2+} current in LNCaP cells to which CaT1 proteins contribute (Vanden Abeele *et al.* 2003) was inhibited by all of our N-terminal rCaT1 fragments (authors' unpublished data).

The inhibition of CRAC activity by the two longer N-termini of rCaT1 is apparently not an unspecific, toxic effect, as endogenous inward rectifier and MagNuM currents of RBL mast cells were not significantly affected by the N_{198}-rCaT1.

Our experiments provide important new insights in the CRAC phenomenon: (i) a contribution of CaT1 to CRAC current is very unlikely, and (ii) a novel mechanism of CRAC channel inhibition by an N-terminal structure of rCaT1. Hence this structure may provide an important tool for identification of molecular candidates of CRAC channels or of components regulating CRAC activity.

References

Bodding M, Wissenbach U & Flockerzi V (2002). The recombinant human TRPV6 channel functions as Ca^{2+} sensor in human embryonic kidney and rat basophilic leukemia cells. *J Biol Chem* **277**, 36656–36664.

Bootman MD, Collins TJ, Peppiatt CM, Prothero LS, MacKenzie L, De Smet P, Travers M, Tovey SC, Seo JT, Berridge MJ, Ciccolini F & Lipp P (2001). Calcium signalling – an overview. *Semin Cell Dev Biol* **12**, 3–10.

Clapham DE, Runnels LW & Strubing C (2001). The TRP ion channel family. *Nat Rev Neurosci* **2**, 387–396.

Cui J, Bian JS, Kagan A & McDonald TV (2002). CaT1 contributes to the stores-operated calcium current in Jurkat T-lymphocytes. *J Biol Chem* **277**, 47175–47183.

Groschner K, Hingel S, Lintschinger B, Balzer M, Romanin C, Zhu X & Schreibmayer W (1998). Trp proteins form store-operated cation channels in human vascular endothelial cells. *FEBS Lett* **437**, 101–106.

Gunthorpe MJ, Benham CD, Randall A & Davis JB (2002). The diversity in the vanilloid (TRPV) receptor family of ion channels. *Trends Pharmacol Sci* **23**, 183–191.

Hamill OP, Marty A, Neher E, Sakmann B & Sigworth FJ (1981). Improved patch-clamp techniques for high-resolution current recording from cells and cell-free membrane patches. *Pflugers Arch* **391**, 85–100.

Harteneck C, Plant TD & Schultz G (2000). From worm to man: three subfamilies of TRP channels. *Trends Neurosci* **23**, 159–166.

Hoenderop JG, Voets T, Hoefs S, Weidema F, Prenen J, Nilius B & Bindels RJ (2003). Homo- and heterotetrameric architecture of the epithelial Ca^{2+} channels TRPV5 and TRPV6. *EMBO J* **22**, 776–785.

Kedei N, Szabo T, Lile JD, Treanor JJ, Olah Z, Iadarola MJ & Blumberg PM (2001). Analysis of the native quaternary structure of vanilloid receptor 1. *J Biol Chem* **276**, 28613–28619.

Kozak JA, Kerschbaum HH & Cahalan MD (2002). Distinct properties of CRAC and MIC channels in RBL cells. *J General Physiol* **120**, 221–235.

Lewis RS (1999). Store-operated calcium channels. *Adv Second Messenger Phosphoprotein Res* **33**, 279–307.

Montell C (2001). Physiology, phylogeny, and functions of the TRP superfamily of cation channels. *Sci STKE* 2001, RE1.

Montell C, Birnbaumer L & Flockerzi V (2002). The TRP channels, a remarkably functional family. *Cell* **108**, 595–598.

Parekh AB & Penner R (1997). Store depletion and calcium influx. *Physiol Rev* **77**, 901–930.

Peng JB, Chen XZ, Berger UV, Vassilev PM, Tsukaguchi H, Brown EM & Hediger MA (1999). Molecular cloning and characterization of a channel-like transporter mediating intestinal calcium absorption. *J Biol Chem* **274**, 22739–22746.

Peng JB, Zhuang L, Berger UV, Adam RM, Williams BJ, Brown EM, Hediger MA & Freeman MR (2001). CaT1 expression correlates with tumor grade in prostate cancer. *Biochem Biophys Res Commun* **282**, 729–734.

Prakriya M & Lewis RS (2002). Separation and characterization of currents through store-operated CRAC channels and Mg^{2+}-inhibited cation (MIC) channels. *J General Physiol* **119**, 487–507.

Putney JW Jr, Broad LM, Braun FJ, Lievremont JP & Bird GS (2001). Mechanisms of capacitative calcium entry. *J Cell Sci* **114**, 2223–2229.

Schindl R, Kahr H, Graz I, Groschner K & Romanin C (2002). Store depletion-activated CaT1 currents in rat basophilic leukemia mast cells are inhibited by 2-aminoethoxydiphenyl borate. Evidence for a regulatory component that controls activation of both CaT1 and CRAC (Ca^{2+} release-activated Ca^{2+} channel) channels. *J Biol Chem* **277**, 26950–26958.

Skryma R, Mariot P, Bourhis XL, Coppenolle FV, Shuba Y, Vanden Abeele F, Legrand G, Humez S, Boilly B & Prevarskaya N (2000). Store depletion and store-operated Ca^{2+} current in human prostate cancer LNCaP cells: involvement in apoptosis. *J Physiol* **527**, 71–83.

Vanden Abeele F, Roudbaraki M, Shuba Y, Skryma R & Prevarskaya N (2003). Store-operated Ca^{2+} current in prostate cancer epithelial cells. Role of endogenous Ca^{2+} transporter type 1. *J Biol Chem* **278**, 15381–15389.

Venkatachalam K, van Rossum DB, Patterson RL, Ma HT & Gill DL (2002). The cellular and molecular basis of store-operated calcium entry. *Nat Cell Biol* **4**, E263–E272.

Voets T, Prenen J, Fleig A, Vennekens R, Watanabe H, Hoenderop JG, Bindels RJ, Droogmans G, Penner R & Nilius B (2001). CaT1 and the calcium release-activated calcium channel manifest distinct pore properties. *J Biol Chem* **276**, 47767–47770.

Wischmeyer E, Lentes KU & Karschin A (1995). Physiological and molecular characterization of an IRK-type inward rectifier K^+ channel in a tumour mast cell line. *Pflugers Arch* **429**, 809–819.

Wissenbach U, Niemeyer BA, Fixemer T, Schneidewind A, Trost C, Cavalie A, Reus K, Meese E, Bonkhoff H & Flockerzi V (2001). Expression of CaT-like, a novel calcium-selective channel, correlates with the malignancy of prostate cancer. *J Biol Chem* **276**, 19461–19468.

Xia Z & Liu Y (2001). Reliable and global measurement of fluorescence resonance energy transfer using fluorescence microscopes. *Biophys J* **81**, 2395–2402.

Xu XZ, Li HS, Guggino WB & Montell C (1997). Coassembly of TRP and TRPL produces a distinct store-operated conductance. *Cell* **89**, 1155–1164.

Xu XZ, Moebius F, Gill DL & Montell C (2001). Regulation of melastatin, a TRP-related protein, through interaction with a cytoplasmic isoform. *Proc Natl Acad Sci U S A* **98**, 10692–10697.

Yue L, Peng JB, Hediger MA & Clapham DE (2001). CaT1 manifests the pore properties of the calcium-release-activated calcium channel. *Nature* **410**, 705–709.

Zitt C, Halaszovich CR & Luckhoff A (2002). The TRP family of cation channels: probing and advancing the concepts on receptor-activated calcium entry. *Prog Neurobiol* **66**, 243–264.

Acknowledgements

We thank S. Buchegger and B. Kenda for excellent technical assistance and I. Graz for establishment of the Fura-2 measurements. This work was supported by projects FWF-F715 (SFB Biomembranes) and FWF-14950 (to K.G.), and FWF-15387, FWF-16537 and ÖNB 9343 (to C.R.)

Author's present address

J.-B. Peng: Division of Nephrology, University of Alabama Birmingham, Birmingham, AL 35294-0000, USA.